Facultad de **Medicina**

GRADO EN CIENCIAS BIOMÉDICAS

TRABAJO FIN DE GRADO

"Cribado de compuestos senolíticos y senomórficos en fibroblastos HDF76 y sus efectos como geroprotectores en C. elegans"

"Screening for senolytic and senomorphic compounds in HDF76 fibroblasts and their effects as geroprotectors in C. elegans"

Autor/a: Sybila Sanguinet Rumayor

Director/a: Markus Schosserer

Co-director/a: Ana Palanca Cuñado

Santander, 8 junio 2025

INDEX

Screening for senolytic and senomorphic compounds in HDF76 and their effects as geroprotectors in C. elegans

GRAPHICAL ABSTRACT

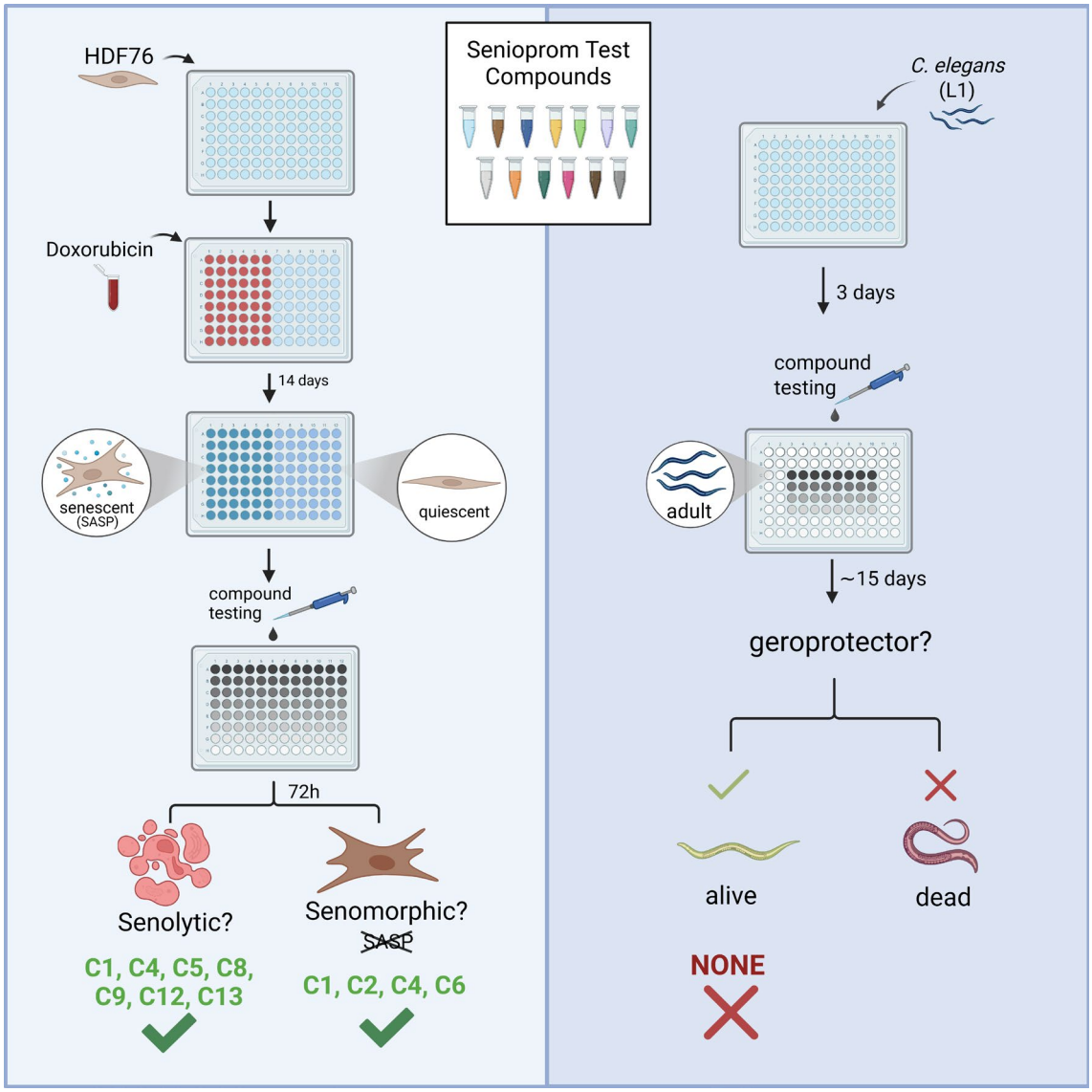

AUTHORS

Sybila Sanguinet Rumayor, Ana Palanca Cuñado, Markus Schosserer

Correspondence: markus.schosserer@meduniwien.ac.at

Trabajo de Fin de Grado
Grado en Ciencias Biomédicas · Facultad de Medicina
2024 – 2025

Screening for senolytic and senomorphic compounds in HDF76 and their effects as geroprotectors in C. elegans

Sybila Sanguinet Rumayor[1,2], Ana Palanca Cuñado[2,3], Markus Schosserer[1*]

[1] Department of Medical Genetics, Medical University of Vienna, 1090 Vienna, Austria
[2] Department of Anatomy and Cell Biology, University of Cantabria, 39011 Santander, Spain
[3] Institute of Biomedicine and Biotechnology of Cantabria (IBBTEC), 39011 Santander, Spain

* Correspondence: markus.schosserer@meduniwien.ac.at

RESUMEN

El envejecimiento es el principal factor de riesgo para muchas enfermedades, y la senescencia celular es un factor clave en este proceso y sus patologías relacionadas. Los senolíticos y senomórficos, que eliminan células senescentes o modulan su fenotipo secretor asociado a la senescencia (SASP), ofrecen un enfoque prometedor para promover una longevidad saludable. El objetivo de este estudio fue evaluar los efectos senolíticos y senomórficos de trece compuestos en fibroblastos dérmicos humanos (HDF76) y sus efectos geroprotectores en *C. elegans*. La senescencia en HDF76 fue inducida usando doxorrubicina y, tras añadir los compuestos, se analizó la actividad senolítica utilizando Zombie NIR y Alamar Blue. Posteriormente, se evaluó la actividad senomórfica mediante ELISA, cuantificando la secreción de IL-6 y MMP1. Además, los compuestos se probaron en *C. elegans* para examinar sus efectos geroprotectores *in vivo*. Los resultados mostraron que los compuestos 1, 4, 5, 8, 9, 12 y 13 exhibieron propiedades senolíticas, mientras que los compuestos 1, 2, 4 y 6 mostraron indicios de actividad senomórfica. Sin embargo, ninguno de los compuestos testados actuó como geroprotector en *C. elegans*. Estudios con tamaños de muestra mayores y concentraciones adicionales son necesarios para confirmar su potencial terapéutico en el envejecimiento y enfermedades relacionadas.

ABSTRACT

Aging is the primary risk factor for many diseases, and cellular senescence is a key factor in this process and its related pathologies. Senolytics and senomorphics, which eliminate senescent cells or modulate their senescence-associated secretory phenotype (SASP), offer a promising approach to promote healthy longevity. The objective of this study was to evaluate the senolytic and senomorphic effects of thirteen compounds in human dermal fibroblasts (HDF76) and their geroprotective effects in *C. elegans*. Senescence in HDF76 cells was induced using doxorubicin and, after treatment with the compounds, senolytic activity was assessed using Zombie NIR and Alamar Blue assays. Then, senomorphic activity was evaluated by ELISA, quantifying IL-6 and MMP1 secretion. Additionally, the compounds were tested in *C. elegans* to examine their geroprotective effects *in vivo*. The results showed that compounds 1, 4, 5, 8, 9, 12 and 13 exhibited senolytic properties, while compounds 1, 2, 4, and 6 showed signs of senomorphic activity. However, none of the compounds tested acted as geroprotectors in *C. elegans*. Further studies with larger sample sizes and additional concentrations are needed to confirm their therapeutic potential in aging and age-related diseases.

KEYWORDS

Cellular Senescence, Senolytics, Senomorphics, Geroprotectors, *C. elegans*, HDF76, Aging, Doxorubicin, Alamar Blue, ELISA

INTRODUCTION

Geroscience proposes that targeting the aging process can significantly improve human health, as aging is the primary risk factor for many diseases[1]. Aging is commonly defined as the functional decline that affects most living organisms over time. It is characterized by a gradual loss of physiological integrity, which leads to an impaired function and increased vulnerability to death[2].

This complex biological process is induced by the accumulation of damage in response to a variety of stressors[3], among many other factors. Some of these cellular and molecular hallmarks of aging include genomic instability, telomere degradation, epigenetic changes, impaired macroautophagy, disrupted nutrient-sensing, proteostasis collapse, cellular senescence, mitochondrial dysfunction, exhaustion of stem cells, impaired intercellular communication, dysbiosis and chronic inflammation[2,4,5].

Of these hallmarks, cellular senescence has been identified as a major contributor of aging and age-related diseases[6]. Cellular senescence is determined by the stable exit from the cell cycle and the loss of proliferative capacity in response to cellular damage and stress[7]. Even though senescent cells (SnCs) are arrested in the cell cycle, they remain metabolically active[7,8]. Many SnCs develop a characteristic senescence-associated secretory phenotype (SASP), secreting factors such as pro-inflammatory cytokines, chemokines, growth factors or matrix metalloproteinases. These factors have the potential to affect the surrounding environment[4].

SnCs tend to accumulate with age, due to both increased induction and decreased clearance by the immune system. Initially, cellular senescence acts as a protective antitumor mechanism where the SASP recruits immune cells to facilitate the removal of SnCs. However, their accumulation overtime contributes to tissue dysfunction. The SASP can alter the behaviour of nearby non-senescent cells, induce secondary senescence and enhance chronic inflammation (inflammaging)[7].

Given the increasing global life expectancy[9], understanding the cellular and molecular mechanism under aging is essential for extending healthspan and improving our quality of life. Targeting senescent cells is a promising approach to mitigate age-related pathologies and improve the overall well-being. To study cellular senescence and aging, researches rely on both *in vitro* and *in vivo* models.

One of the most commonly used *in vitro* cell models are skin fibroblasts. These cells are especially relevant for senescence studies, as they are the main cell type in the dermis, a tissue where aging signs appear early and senescent cells accumulate noticeably. In addition, they have a limited replicative lifespan and are easy to culture and manipulate, making them ideal for functional studies of novel compounds[10]. In this study, primary human dermal fibroblast (HDF76) were used.

In addition to cell culture models, *Caenorhabditis elegans* (*C. elegans*) serves as an important *in vivo* model for aging research. This nematode shares 60-80% genetic homology with humans, has high fertility rates and a short lifespan (approximately 18-20 days), making it ideal for longevity studies[11]. Moreover, several pathways modulating the aging process have proven to be highly conserved from *C. elegans* to humans[12].

Previous studies have highlighted the potential of senotherapeutics, such as senolytic and senomorphic compounds, in targeting cellular senescence and promoting healthy longevity[13–15]. On the one hand, senolytics are designed to selectively eliminate

senescent cells by inducing apoptosis. On the other hand, senomorphics suppress the effects of the SASP without causing cell death, modulating the inflammatory environment surrounding senescent cells[1].

However, despite promising findings in preclinical models, the therapeutic potential of many senotherapeutic compounds remains uncertain due to side effects and variable efficacy[16]. As a result, further investigation into new compounds with potential anti-aging properties is essential.

To address this need, the present study focuses on a set of compounds initially identified through screens *in silico*. Moreover, these compounds have shown promising efficacy in a previous senescence-like model by our cooperation partners. However, it is still unclear whether they exhibit senolytic or senomorphic activity in human cells such as HDF76, or whether they can have broader geroprotective effects (delaying or reversing aging processes, thus extending lifespan and healthspan[17]) in *C. elegans*.

Our primary objective is to evaluate the potential senolytic and senomorphic effects of these compounds in human dermal fibroblasts HDF76 and to evaluate their geroprotective effects in *C. elegans*.

It is expected to see that some of the tested compounds will reduce or stabilize cellular senescence in HDF76 cells and promote lifespan extension in *C. elegans*, thus acting as potential geroprotectors.

The identification of effective compounds will not only advance our understanding of cellular senescence but also pave the way for future research on geroprotector substances aimed at promoting healthy aging and improving the quality of life.

RESULTS

Senolytic Assessment

The first objective was to assess the potential senolytic activity of test compounds. To achieve that goal, Zombie NIR was used to evaluate cell death in senescent and quiescent HDF76 after treatment.

Senescence was induced by two rounds of doxorubicin treatment. After 14 days, senescent and quiescent cells were exposed to different test compounds for 72 hours. Zombie NIR dye staining was then used to distinguish live (Zombie−) from dead (Zombie+) cells.

The results indicated that treatment with compound 6 at concentrations equal or greater than 1.25µM resulted in 100% of senescent and quiescent cells being Zombie+, suggesting a non-selective cytotoxic effect at higher doses (Figure 1A).

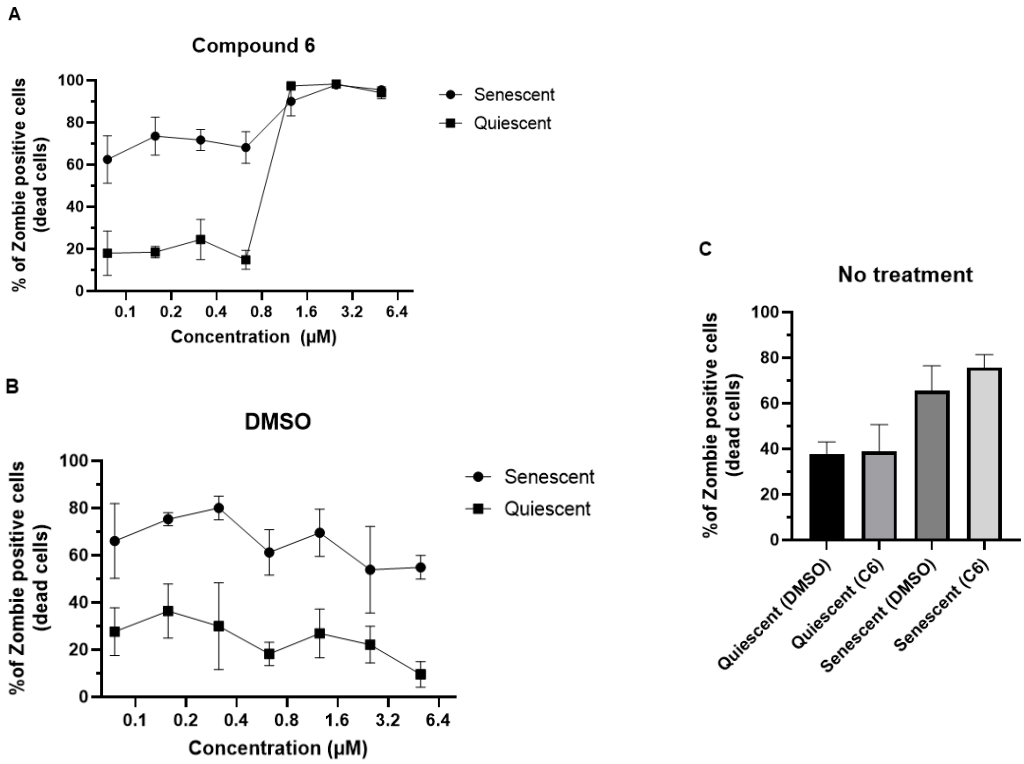

Figure 1. Evaluation of cell death in senescent and quiescent HDF76 using Zombie NIR.

(A) Line graph showing cell death in senescent and quiescent cells after a 72-hour treatment with compound 6 at increasing concentrations. Cell death was assessed by flow cytometry using Zombie NIR dye, which labels cells with compromised membrane integrity (Zombie+). **(B)** Line graph showing the Zombie+ senescent and quiescent cells in the DMSO control. **(C)** Bar graph showing the baseline levels of Zombie+ cells measured in untreated senescent and quiescent cells.

When focusing on all concentrations below 1.25µM, the data revealed that more than 60% of senescent cells were Zombie+, suggesting a high rate of cell death. In contrast, only around 20-30% of quiescent cells were positive for Zombie NIR under the same

conditions, indicating that the compound may preferentially affect senescent cells (Figure 1A). However, when comparing these results to the DMSO control, the percentage of Zombie+ cells was similar; 60-70% for senescent cells and 20-30% for quiescent cells (Figure 1B). These results suggest that the observed cell death in treated cells may not be to the compound itself.

Further analysis showed that untreated cells also exhibited a high level of zombie+ staining (around 60-80% for senescent cells and 40% for quiescent cells) (Figure 1C). These findings highlight a high Zombie+ signal in senescent cells regardless of compound treatment, raising concerns about the specificity of the assay in this context.

Compounds 1, 4, 5, 8, 9, 12 and 13 showed signs of senolytic activity

Given the limitations observed with the Zombie NIR dye, the Alamar Blue assay was used as an alternative method to evaluate cell viability. Again, the aim was to identify compounds capable of selectively reducing survival in senescent cells without affecting quiescent ones.

Doxorubicin was used to induce senescence in HDF76. After 14 days, senescent and quiescent cells were treated with the test compounds for 72 hours. Then, Alamar Blue was added and absorbance at 570 and 600nm was measured. The Alamar Blue reagent has a component that changes colour in metabolically active cells, allowing indirect measurement of cell viability.

Among the compounds tested, numbers 2, 3, 6, 7, 10 and 11 did not show selective senolytic activity at the concentrations evaluated. Compound 2 exhibited a non-specific cytotoxic effect at concentrations ≥20μM, reducing viability in both senescent and quiescent cells. At concentrations ≤10μM, compound 2 had no effect (Figure 2A).

Compound 3 demonstrated a clear toxic effect at concentrations ≥320μM, with complete loss of viability in senescent and quiescent fibroblast. At concentrations below 80μM, both cell types maintained high viability. At 160μM, a slight reduction in senescent viability was observed (~55%), while quiescent cells remained near 85%. However, this difference did not appear to be meaningful (Figure 2B).

For compound 6, strong cytotoxicity was presented in all tested conditions, with viability dropping below 10% for both senescent and quiescent cells (Figure 2C).

Compound 7 caused cell death at concentrations above 5μM, whereas at 1.25 and 2.5μM, viability remained high (>80%) in both cell types, suggesting no selective effect (Figure 2D).

Compound 10 did not show any effect at concentrations ≤160μM. At 320μM, a drop in viability was noted in senescent cells (~55%), while quiescent cells remained at 80%. Nevertheless, this difference was not significant ($p>0.05$, Unpaired t test with Welch's correction) (Figure 2E).

Lastly, in the case of compound 11, both populations maintained high survival at doses ≤3.75μM. At higher levels, viability decreased similarly and no clear difference was detected between treated and control groups (Figure 2F).

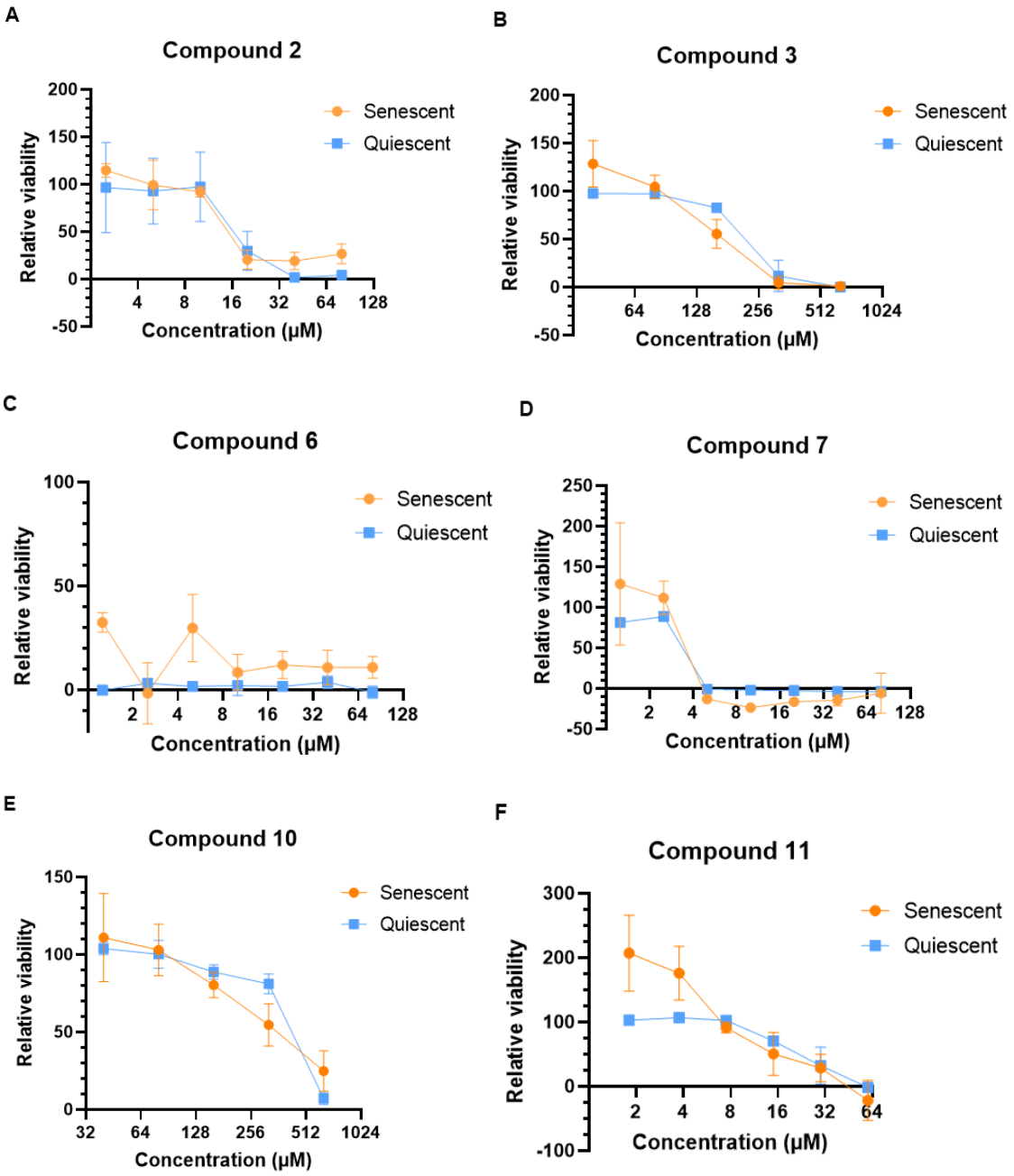

Figure 2. Alamar blue assay

Line graph showing the relative viability of senescent and quiescent HDF76 after treatment with compounds **(A)** 2, **(B)** 3, **(C)** 6, **(D)** 7, **(E)** 10 and **(F)** 11. Cell viability was assessed using Alamar Blue. In these compounds, no clear senolytic effect was found at the concentrations tested.

In contrast, compounds 1, 4, 5, 8, 9, 12 and 13 revealed signs of senolytic activity. For compound 1, a clear trend was observed in which quiescent cells consistently maintained higher viability than senescent cells. This difference was particularly marked at 320μM, where quiescent cell viability was around 70%, while senescent dropped to 15%. Similarly, at 160μM, quiescent cells remained near 80%, and senescent cells around 50%. At the highest dose tested (640μM), signs of toxic effects started to appear, with senescent viability droping to 0% and quiescent to 40%. No effect was detected at concentrations below 80μM, where survival remained above 80% in both cell types (Figure 3A).

In compound 4, senescent cell viability appeared consistently lower than that of quiescent cells across the tested concentrations. This difference became relevant specially at 160 and 320μM, where viability levels differed by approximately 25-35% (Figure 3A).

Compound 5 had no effect on viability at concentrations ≤40μM. However, at 80μM, the viability of senescent cells dropped to less than 10% while that of quiescent cells was maintained around 70% (Figure 3C).

Compound 8 also presented promising results. In both cell types, viability remained at 100% at concentrations ≤ 2.5μM, and dropped at 40μM. At intermediate concentrations, a progressive loss of viability was observed in senescent cells while quiescent cells remained unaffected. For instance, at 5μM senescent cell viability decreased to ~80%, at 10μM to ~70%, and at 20μM senescent viability reached 0%. At all of those concentrations, quiescent cells maintained 100% viability (Figure 3D).

Similarly, compound 9 showed no effect up to 5μM, and non-specific cytotoxicity at ≥20μM. However, at 10μM, viability in senescent cells was reduced to approximately 6%, while that of quiescent cells remained at 100% (Figure 3E).

Compound 12 reduced viability in both cell types at high concentrations (≥40μM), suggesting non-specific toxicity. At lower concentrations (2–20μM), the compound reduced the viability of senescent cells (~40-50%) compared to quiescent cells (~80%) (Figure 3F).

Finally, a similar pattern was observed in compound 13, where viability was reduced in both cell types at concentrations ≥20μM. Nevertheless, at lower doses, a significant difference was observed. At 5μM, senescent cell viability was approximately 50%, while quiescent remained at 70%. Also, at 10μM, senescent viability dropped to 35% whereas quiescent cells maintained a level near 61% (Figure 3G).

The DMSO controls reflected high cell viability across all concentrations tested (Figure S1).

Overall, half of the tested compounds either had no effect or caused non-specific cytotoxicity at the concentrations used. In contrast, compounds 1,4, 5, 8, 9, 12 and 13 selectively reduced the viability of senescent cells without affecting quiescent cells, suggesting potential senolytic activity.

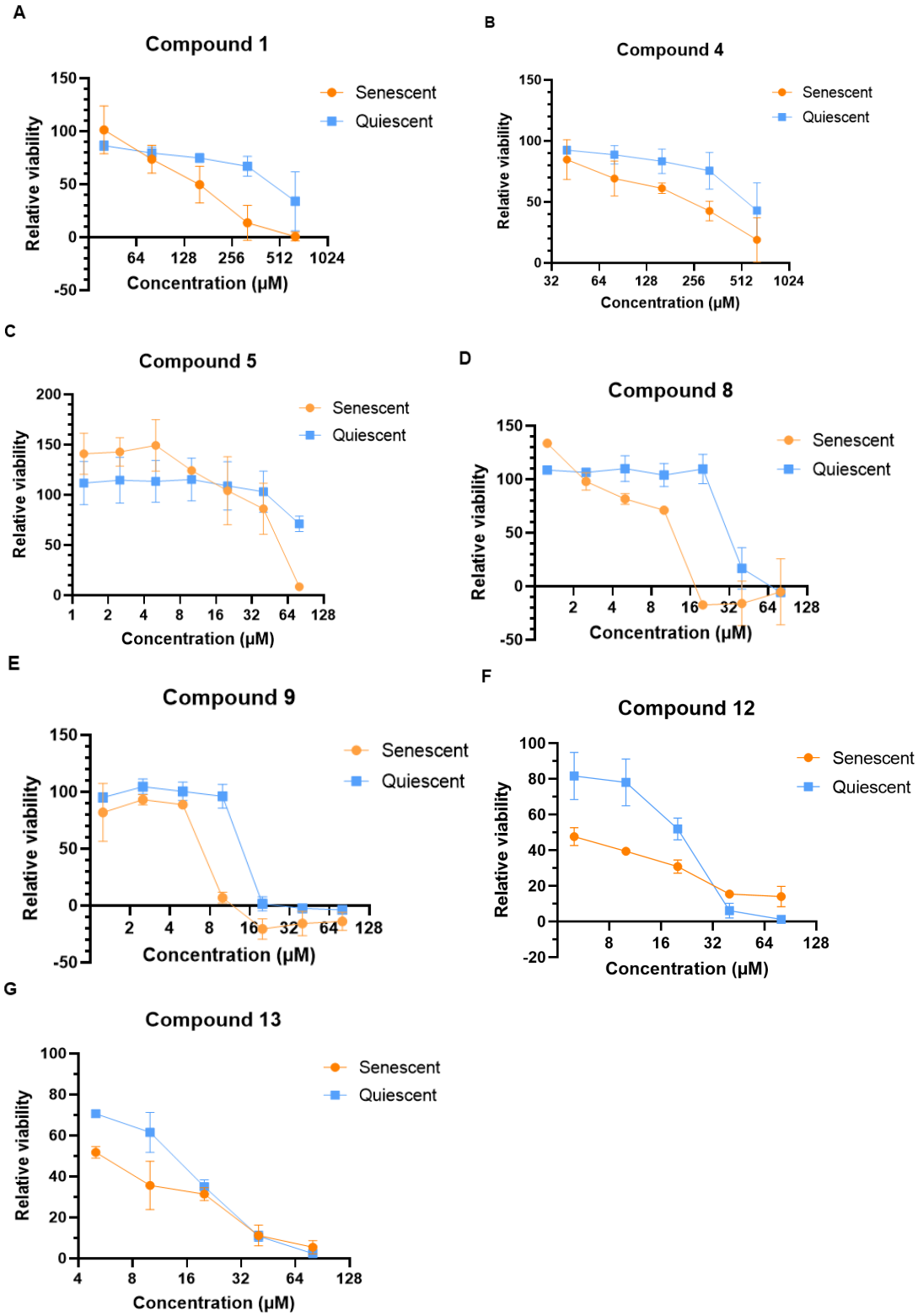

Figure 3. Alamar blue assay.

Line graph showing the relative viability of senescent and quiescent HDF76 after treatment with compounds **(A)** 1, **(B)** 4, **(C)** 5, **(D)** 8, **(E)** 9, **(F)** 12 and **(G)** 13. Cell viability was assessed using Alamar Blue. In these compounds, signs suggestive of senolytic activity were observed.

Compounds 1, 2, 4 and 6 showed signs of senomorphic activity

To assess the potential senomorphic effects of the test compounds, secretion levels of Interleukin-6 (IL-6) and Matrix Metalloproteinase-1 (MMP1) in senescent cells were quantified using ELISAs.

Supernatants of senescent cells were collected after 72 hours of treatment. Then, the levels of these two factors present in the SASP were measured with ELISAs in technical duplicates.

Regarding IL-6 secretion, most compounds did not produce a consistent reduction compared to DMSO-treated cells. For instance, compound 3 showed similar IL-6 levels between treated and control senescent cells (Figure 4C). In addition, compound 2 did not present any signs of reduced IL-6 levels at the tested concentrations. Interestingly, an increase was observed at 5µM (Figure 4B).

Similarly, compounds 7, 8, 9, 10, 11, 12 and 13 failed to demonstrate a consistent decrease in IL-6 secretion (Figures 4F, 4G, 4H, 4I, 4J, 4K and 4L). In several cases, IL-6 levels in treated senescent cells were higher than those in control groups. Overall, a high degree of variability was noted among these compounds.

Nevertheless, three compounds showed trends towards reducing IL-6 secretion, suggesting possible senomorphic effects. Compound 1 appeared to markedly decrease IL-6 levels in treated senescent cells, with concentrations around 200–250 pg/mL compared to approximately 800 pg/mL in DMSO-treated controls (Figure 4A). Likewise, compound 4 pointed towards a lower IL-6 secretion, with treated cells having around 550-650 pg/mL versus 800 pg/mL in controls (Figure 4D). Additionally, senescent cells treated with compound 6 exhibited tendencies towards lower IL-6 levels (1500pg/mL) relative to DMSO controls (2000pg/mL) (Figure 4E). Further experiments with biological triplicates are necessary to confirm statistical significance of these observations.

Concerning MMP1 secretion, compounds 3, 4, 7, 8, 9, 10 and 11 showed similar levels between compound-treated and control cells, ranging between 70-100 pg/mL (Figures 5C, 5D, 5F, 5G, 5H, 5I and 5J). For compounds 12 and 13, MMP1 signal appeared to increase compared to DMSO controls (Figures 5K and 5L).

In contrast, compound 1 appeared to exhibit senomorphic activity. There was a slight reduction of MMP1 in treated cells at 40µM and a more pronounced decrease at 80µM (Figure 5A). Moreover, for compound 2, the analysis suggests a potential senomorphic effect at 10µM, as it was the only concentration at which MMP1 levels appeared to decrease. No apparent effect was observed at lower concentrations (Figure 5B). Finally, compound 6 also appeared to have senomorphic activity. At 0.7µM, MMP1 secretion in compound treated senescent cells was approximately 65 pg/ml, while the DMSO treated control was around 100 pg/mL (Figure 5E). Additional experiments are necessary to assess statistical significance.

In summary, these findings suggest that compounds 1, 4, and 6 reduce IL-6 levels, while compounds 1, 2, and 6 reduce MMP1 levels. Notably, both compound 1 and compound 6 decreased the secretion of both IL-6 and MMP1, further supporting their potential senomorphic activity.

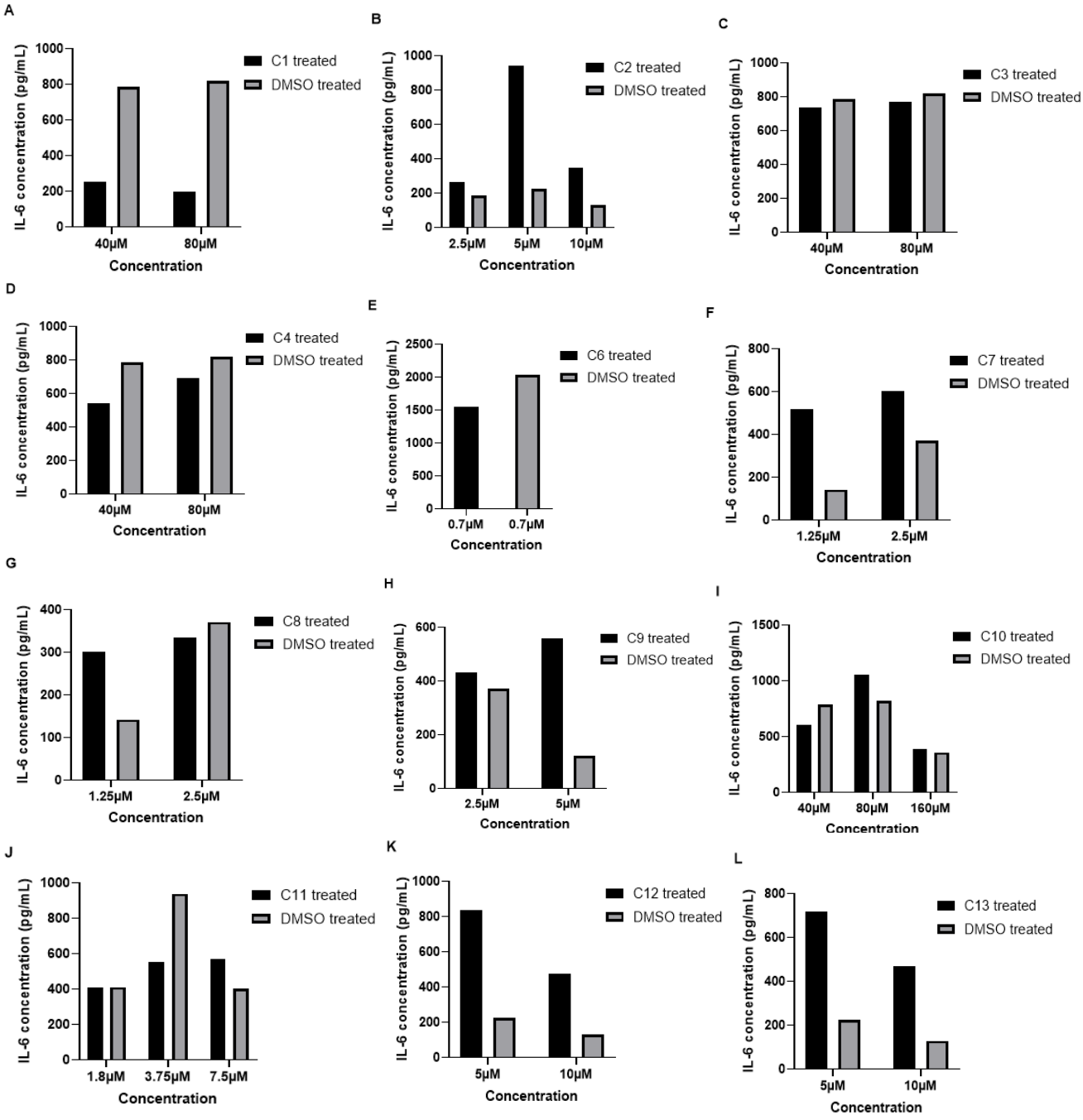

Figure 4. IL-6 secretion in senescent HDF76.

Bar graph showing IL-6 concentration secreted by senescent cells treated with compounds **(A)** 1, **(B)** 2, **(C)** 3, **(D)** 4, **(E)** 6, **(F)** 7, **(G)** 8, **(H)** 9, **(I)** 10, **(J)** 11, **(K)** 12 and **(L)** 13 and their respective DMSO controls. IL-6 levels were quantified using ELISA.

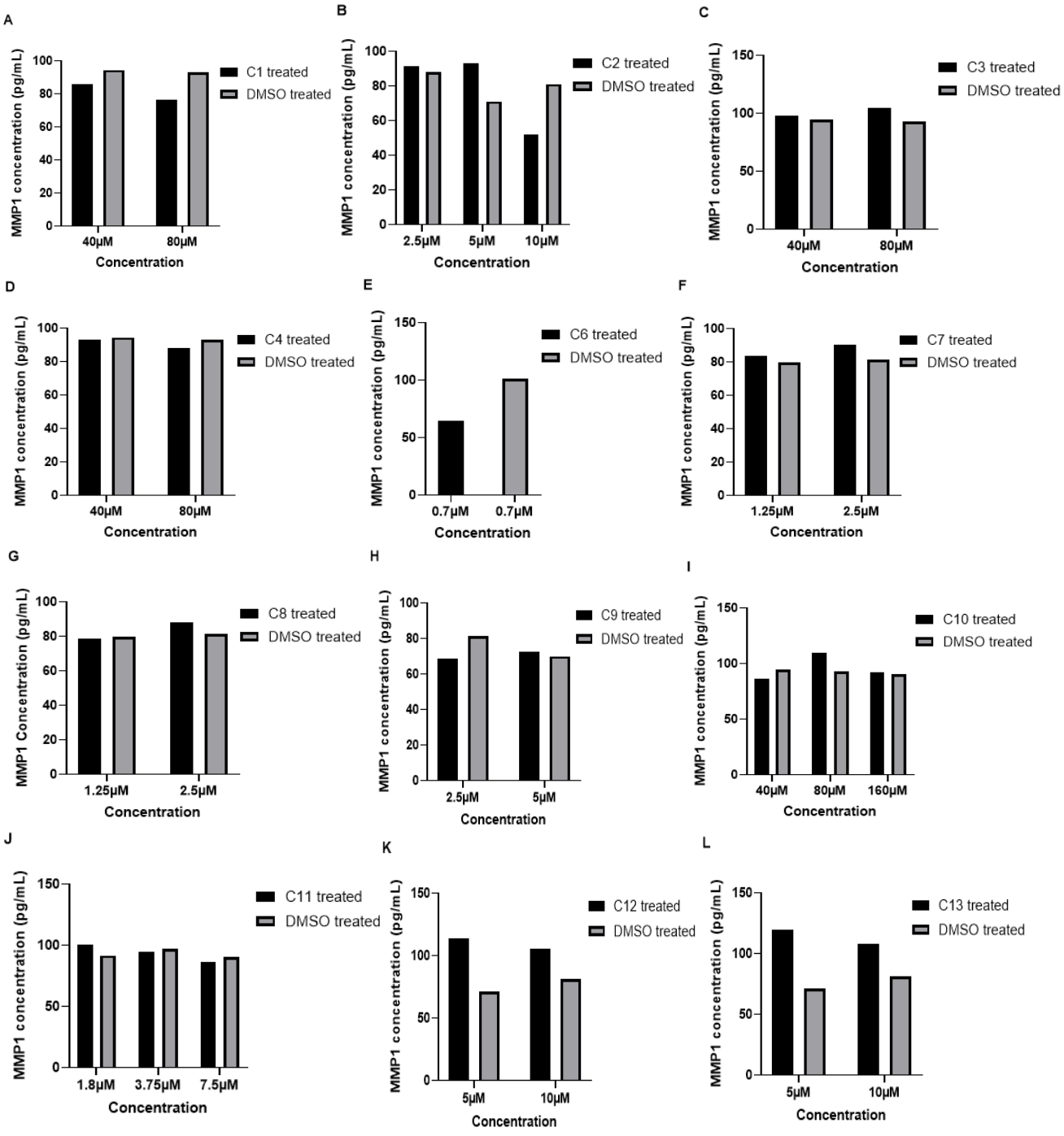

Figure 5. MMP1 secretion in senescent HDF76.

Bar graph showing MMP1 concentration secreted by senescent cells treated with compounds **(A)** 1, **(B)** 2, **(C)** 3, **(D)** 4, **(E)** 6, **(F)** 7, **(G)** 8, **(H)** 9, **(I)** 10, **(J)** 11, **(K)** 12 and **(L)** 13 and their respective DMSO controls. MMP1 levels were quantified using ELISA.

None of the tested compounds demonstrated clear geroprotective effects in *C. elegans*

To evaluate the potential geroprotective effect of the tested compounds, survival assays were performed in *C. elegans* TJ1060. This strain has two temperature-sensitive mutations that make the worms completely sterile at 25ºC. Synchronized adult worms were treated with some of the test compounds at three different concentrations (250µM, 50µM and 10µM). Then, viability was assessed every 2-3 days by monitoring movement under the microscope.

In the first experiment, all worms died prematurely (by day 9 regardless of treatment) due to excessive temperature in the incubator (Figure S2). These conditions were considered unsuitable for evaluating compound effects and were excluded from further interpretation.

Following the observations on the first experiment, temperature was reduced and *C. elegans* survival in control conditions followed an expected pattern (living approximately 18-19 days). However, a substantial number of worms disappeared from the wells over time. Therefore, median survival, defined as the time point at which 50% of worms remained alive, was used as a reference for comparing treatment groups.

In the second experiment (E2), at the highest concentration (250µM), all of the tested compounds showed signs of general toxicity. The median survival occurred on day 6, 3, 9 and 4 for compounds 6, 7, 8 and 9 respectively. These were considerably earlier than the DMSO control group, which reached 50% survival around day 13. Moreover, all worms treated with compound 7 or compound 8 died by day 11, suggesting strong toxicity at this dose for those compounds (Figure 6A).

At 50µM, a similar trend was observed. DMSO control groups reached the 50% survival on day 16. However, worms treated with compound 9 reached this point on day 11, and the ones treated with compound 7 on day 4. In addition, compound 7-treated worms were all dead on the 11th day, suggesting toxic effects at this concentration. For compound 8, the median survival was undefined due to extensive worm loss. For compound 6, the median was reached on day 13. Survival curves for compounds 6 and 8 did not differ significantly from the DMSO control ($p > 0.05$, Log-rank (Mantel-Cox) test) (Figure 6B).

At 10µM, compound-treated groups still did not outperform controls. This dose with compound 7 seemed to be toxic for worms, with the median survival occurring on day 9. Furthermore, in compounds 6 and 8 the 50% survival was reached on day 11, the same as the DMSO control, but the curves were not different ($p>0.05$, Log-rank (Mantel-Cox) test). Lastly, compound 9 had a slightly longer median survival (day 16), but this difference was not statistically significant ($p > 0.05$ Log-rank (Mantel-Cox) test) (Figure 6C).

In the third experiment, at 250µM, all treatment groups reached the median survival between days 2 and 6. Notably, the DMSO control also reached median survival on day 2, suggesting an issue with the plates or environmental conditions. Only compound 13 showed a statistically significant difference compared to DMSO ($p < 0.05$ Log-rank (Mantel-Cox) test), though this was associated with toxicity rather than increased survival (Figure 6D).

At 50μM, there was a high worm loss, especially in the DMSO control, where the median survival was not reached. For compound 10, it was also undefined due to missing worms. Lastly, compounds 12 and 13 reached median survival around days 10-11. When a statistical analysis was performed, none of the survival curves differed significantly from the DMSO control curve ($p>0.05$, Log-rank (Mantel-Cox) test) (Figure 6E).

Finally, at 10μM, the median survival for the DMSO control was day 11, the same as compounds 10 and 13. Compound 12 had a slightly bigger median survival (day 13), but the difference was not statistically significant ($p > 0.05$ Log-rank (Mantel-Cox) test), meaning the survival curves were not different (Figure 6F).

To sum up, none of the compounds tested at 250, 50, or 10μM clearly extended lifespan in *C. elegans* compared to controls.

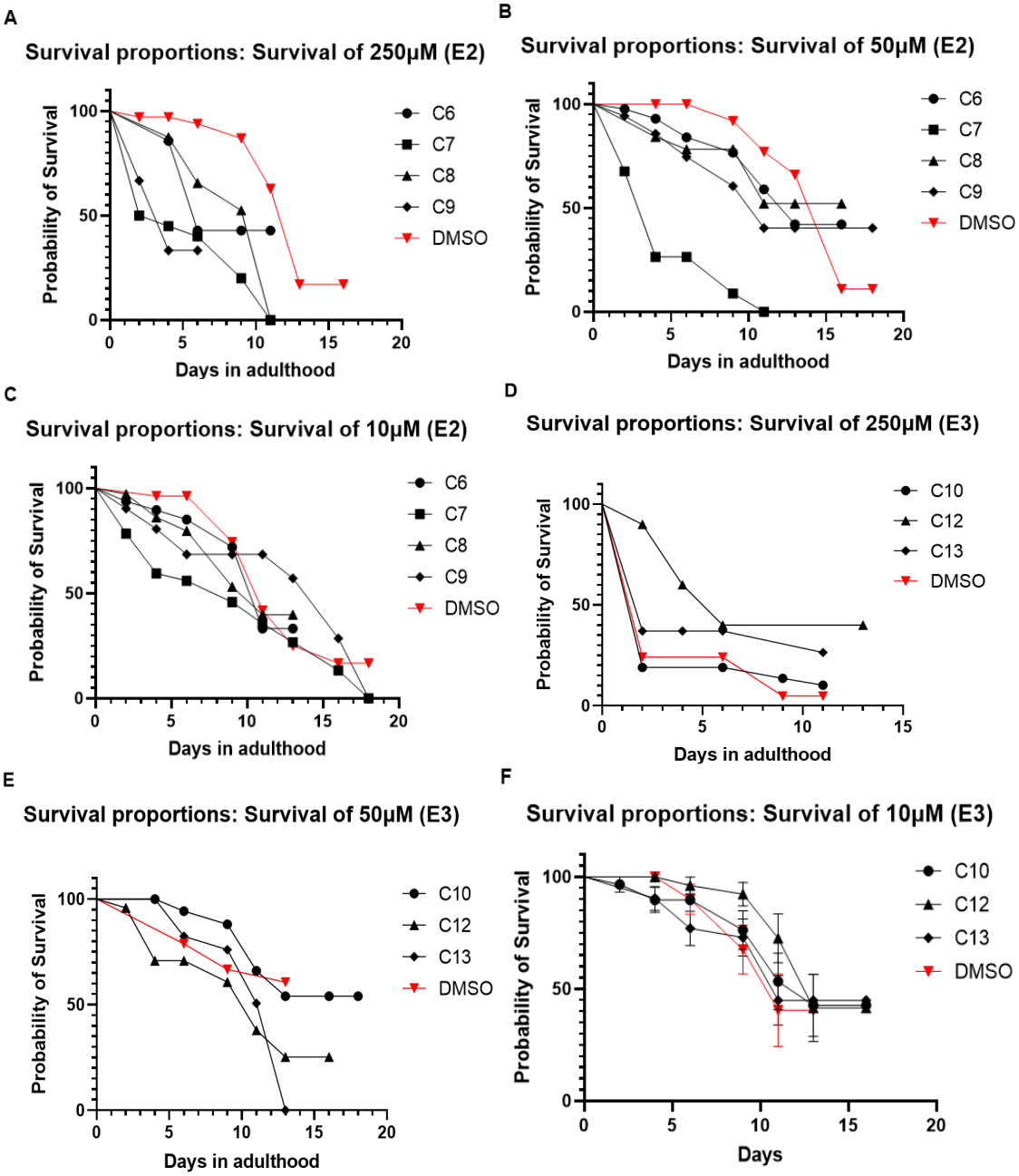

Figure 6. Survival curves of *C. elegans*.

Line graphs showing the survival of C. elegans in the second and third experiments, where the temperature was maintained at 25°C. In Experiment 2, worms were treated with compounds 6, 7, 8, and 9 at **(A)** 250µM, **(B)** 50µM, and **(C)** 10µM. In Experiment 3, worms were treated with compounds 10, 12, and 13 at concentrations **(D)** 250µM, **(E)** 50µM, and **(F)** 10µM.

DISCUSSION

In the initial screening, Zombie NIR results showed non-selective cytotoxicity with compound 6 at concentrations ≥1.25μM. At lower concentrations, high percentage of cell death was showed in senescent cells, while quiescent cells remained relatively unaffected. However, when checking the DMSO control, a similar level of cell death was observed, despite DMSO not being toxic at these concentrations[18]. This suggests that the observed effects may not be due to the compound. In the non-treated condition, senescent cells displayed the same high percentage of cell death.

Previous literature indicates that senescent cells exhibit changes in membrane composition, which results in increased permeability[19,20]. This could potentially explain the high cell death detection. It is possible that Zombie NIR dye is able to penetrate the membrane in live cells due to their altered composition and stain not only surface proteins, but also cytosolic ones. This could lead to a false positive of Zombie+ signal, detecting cells as dead even when they are still alive.

Given these findings, Zombie NIR dye is not a good method for detecting cell death in our screening model. The dye binds to senescent cells, which have altered membrane properties, and this results in a false signal. A more reliable method was needed to assess cell viability in our experiments.

Moving from the Zombie NIR results, we next examined cell viability with the Alamar Blue assay. Among the compounds tested, number 2, 3, 6, 7, 10, and 11 did not exhibit selective senolytic activity at the tested concentrations. For most of them, non-specific citotoxicity was found at the higher concentrations tested and no effect at the lower ones. Compound 6 demonstrated a strong toxicity at all concentrations tested, which is consistent with the results from the Zombie NIR assay, where compound 6 also showed toxicity at ≥1.25μM.

In contrast, compounds 1, 4, 5, 8, 9, 12 and 13 showed signs suggestive of senolytic activity. Compound 1 significantly reduced viability in senescent cells compared to quiescent cells, specially at 320μM. Similarly, compound 4 showed lower viability in senescent at 160 and 320μM. Compound 5 seemed to have selective senolytic activity at 80μM. Compound 8 also exhibited a strong dose-dependent effect, with viability of senescent dropping at 20μM. Then, compound 9 reduced senescent cell viability compared to quiescent cells at 10 μM. Compound 12 and 13 showed similar trends, both of them showing a potential senolytic effect at lower doses (<10μM).

The DMSO controls maintained high cell viability across all concentrations tested, confirming that DMSO alone did not affect the cells and that any observed reduction in viability was related to the compounds themselves, rather than solvent toxicity.

Overall, these findings indicate that several compounds exhibited promising trends towards senolytic activity. However, further studies are necessary to confirm these findings and exactly define the concentration window in which this compounds act.

After analysing the Alamar Blue data, ELISA assays were performed to evaluate the secretion of two SASP factors (IL-6 and MMP1), in treated-senescent HDF76. Regarding IL-6 secretion, most compounds did not produce a consistent reduction compared to DMSO-treated cells. In some cases, IL-6 levels in treated senescent cells were higher than those in control groups. This increase could be linked to cellular stress, which has

been shown to control cytokine synthesis[21]. Moreover, senescent cells exhibit an altered stress response that can further amplify the SASP upon stress exposure[22]. A possible explanation is that the compound induced cellular stress, leading to an increase in cytokine synthesis, which subsequently resulted in the higher IL-6 signal detected.

Three of the compounds (compounds 1, 4, and 6) showed trends towards reducing IL-6 secretion, which may indicate potential senomorphic activity. Interestingly, compound 6 exhibited a higher total amount of IL-6 secretion. This could be explained by the higher cell density, as cells were seeded at nearly three times the concentration of the other compounds.

Concerning MMP1 secretion, compounds 3, 4, 7, 8, 9, 10, and 11 showed similar levels compared to control senescent cells, indicating no clear senomorphic effect. Compounds 12 and 13 appeared to increase MMP1 secretion compared to DMSO controls. This increase may be again associated with a stress response.

Compounds 1, 2 and 6 seemed to reduce MMP1 levels in senescent cells. Compound 1 showed a slight effect at 40 and 80μM, compound 2 at 10μM and compound 6 at 0.7μM, suggesting senomorphic effects at these concentrations.

There was a high degree of variability noted in the DMSO controls. This could be attributed to the heterogeneous nature of senescent cells, which can lead to differences in cytokine secretion even under the same experimental conditions. Furthermore, the variability could be also explained due to differences in the number of cells seeded in each well.

These results indicate that while some compounds show promising trends towards senomorphic activity, further research is needed to confirm their real effects. Additional experiments testing more concentrations and using biological triplicates are necessary to confirm the statistical significance of these observations.

Finally, taking a look into the survival assays in *C. elegans*, in the first experiment, worms died prematurely by day 9. The incubator was set to 27°C, which is slightly above the optimal 25°C for the TJ1060 strain. Previous studies have shown that higher temperatures generally reduce the lifespan of *C. elegans* and other ectotherms[23]. This suggests that the temperature in our incubator likely accelerated the aging process, and therefore, survival was altered. These results were excluded from further analysis. The temperature was then adjusted to 25°C, and two additional experiments were conducted.

The findings of the following experiments demonstrated that most compounds exhibited non-specific toxicity at higher concentrations but did not show significant effects at lower doses. Compound 7 appeared to be toxic at all concentrations tested, needing further investigation at lower doses. Compound 9 displayed toxicity at 250 and 50μM. For the rest of the compounds, toxicity was only observed at the highest concentration.

Surprisingly, at 250μM in the third experiment, the median survival of the DMSO control was day 2, which was unusual since we previously demonstrated that DMSO was not toxic at this concentration. Old agar plates were used in this experiment, which may have affected the viability of the worms. Additionally, it is possible that the bleaching protocol did not work as expected, leaving some dead bodies in the wells which could have been misclassified as dead during the analysis.

Overall, none of the compounds showed a significant effect on worm lifespan extension, indicating that none of the tested compounds clearly acted as geroprotectors at the concentrations evaluated.

The experiments faced some limitations. There was a high rate of worm loss in the wells, which reduced the reliability of the results. Moreover, the possible issues with the bleaching technique may have contributed to the observed variability.

Future experiments should address the current limitations by using larger sample sizes and testing different concentrations of the compounds to fully evaluate their potential geroprotective effects.

In conclusion, the results from Zombie NIR, Alamar Blue, ELISA, and *C. elegans* assays collectively suggest that while several compounds exhibited promising trends towards senolytic or senomorphic activity, further investigation is needed to confirm the findings. Overall, this study provides valuable insight into the potential of these compounds as therapeutic agents, but more work is necessary to fully assess their efficacy and mechanisms of action.

METHODS

Cell Screening

Cell Culture and Senescence Induction

Ensuring proper cell growth and maintenance during experiments was essential. Human Dermal Fibroblasts (HDF) were cultured in Dulbecco's Modified Eagle Medium F12 (DMEM F12) (D6421, Sigma-Aldrich). This medium was supplemented with 10% heat-inactivated Fetal Calf Serum (FCS) (A5256701, GIBCO) to supply essential growth factors, 1 g of Primocin (ant-pm-2, InvivoGen) per 20 mL of solution to prevent microbial contamination and L-Glutamine (G7513, Gibco) to support optimal cell metabolism and proliferation. Hereafter, this formulation will be referred as F-12.

Before starting, HDF76 were seeded in 96 well plates at a density of around 2000 cells per well to ensure optimal cell adhesion and growth prior to the treatment. The cell concentration was determined using the Luna II cell counter.

The first day, senescence was induced *in vitro* by exposing fibroblasts to F-12 medium containing a final doxorubicin hydrochloride (D1515, Sigma-Aldrich) concentration of 150nM. Cells were incubated at 37°C for 72 hours. After that, the treatment was repeated using freshly prepared doxorubicin-containing media to ensure the senescence transformation, followed by another incubation at 37°C for 72 hours.

Following the doxorubicin treatment, cells underwent a recovery phase to allow the establishment of a stable senescent phenotype by replacing the media with fresh F-12 under standard conditions. On day 14, senescence induction was confirmed by assessing characteristic morphology, including enlargement, flattening and loss of proliferation[24].

Compound Testing

After confirming the successful induction of senescence, cells were ready to be treated with the test compounds. The old medium was removed and cells were washed twice with Phosphate Buffered Saline (PBS). Each compound was diluted in F-12 medium at the appropriate concentrations. Then, 100 µL of the solution were added to each well.

The same treatments were applied to both senescent and quiescent cells to allow a direct comparison of their effects. Each condition was tested in triplicate to ensure the reproducibility and statistical robustness of the results. A Dimethyl Sulfoxide (DMSO) control was also included to account for potential solvent-related cytotoxicity. Plates were incubated at 37 °C for 72 hours and then cell viability was assessed.

Zombie NIR Dye and FACS Analysis

Following the three days of treatment, cell death was assessed using Zombie NIR Fixable viability Kit (423106, BioLegend).

The Zombie dye binds to amine groups on proteins and emits red fluorescence when excited at 633 nm. In viable cells, the dye is excluded due to intact membranes, resulting in minimal labelling of surface proteins. In contrast, the dye is permeant in non-viable cells with compromised membranes, labelling not only surface proteins, but also cytoplasmatic and nuclear proteins. Thus, dead cells show a significantly higher fluorescent signal compared to live cells [25].

The Zombie dye allowed clear discrimination between live (Zombie-) and dead (Zombie+) cells during flow cytometry analysis. This was relevant because it enabled the quantification of compound-induced cytotoxicity, helping to evaluate whether the tested compound had a senolytic effect.

For the experiment, first, the culture medium from each well was transferred to a V-bottom 96-well plate for easier centrifugation. After centrifugating 350 rpm for 5 minutes, 100 µL of supernatant was collected and stored for later ELISA analysis.

Cells were then washed with PBS, and the buffer transferred to the V-bottom plate. The plate was centrifuged again at 350 rpm for 5 minutes and the supernatant was discarded. Next, 50 µL of StemPro Accutase Dissociation Reagent (A1110501, Gibco) was added to detach the cells, incubated for 3–5 minutes at 37ºC, and stopped by adding 150 µL of F-12 culture medium. The full cell suspension was transferred to the V-bottom plate and centrifuged at 350 rpm for 5 minutes. The supernatant was discarded.

To properly calibrate the cytometer and define gating parameters for Zombie staining, four control conditions were included. One well was stained with Zombie NIR only, another with DAPI only, and a third was left unstained to assess background fluorescence. The fourth well was used to create a 50:50 mix of live and dead cells to help distinguish between Zombie+ and Zombie- populations. To generate dead cells, half of the sample was incubated at 60 °C for 10 minutes in a thermoblock and then transferred into ice for two minutes.

For staining, Zombie dye was diluted 1:1000 in PBS. The pellets were resuspended in 100 µL of the diluted dye and incubated for 15 minutes at room temperature, protected

from light. Samples were then centrifuged at 400 rpm for 5 minutes and the supernatant was discarded.

To fix the cells, 200 µL of cold methanol was added. After a 15-minute incubation protected from light, samples were centrifuged at 400 rpm for 5 minutes. The supernatant was removed. Finally, the cells were resuspended in 200 µL of PBS and stored at 4 °C until analysis.

For nuclear staining, DAPI (62248, Thermo Fisher Scientific) was used. Cells were first centrifuged at 400 rpm for 5 minutes, and the supernatant was discarded. DAPI was diluted 1:50 in wash Buffer and 150 µL were added to resuspend the pellet. Samples were incubated 15 minutes at room temperature, protected from light. Afterwards, cells were centrifuged again at 400 rpm for 5 minutes. The supernatant was discarded, and the pellet was resuspended in 150 µL of washing buffer for flow cytometry analysis.

Alamar Blue

The alamarBlue Assay is designed to assess the metabolic activity and proliferation of different cell lines, bacteria, yeast, fungi and protozoa[26]. For this study, this technique was particularly valuable to determine cell viability after treatment.

The principle of the AlamarBlue assay is based on an oxidation-reduction (REDOX) indicator that detects cellular metabolic activity. Its active compound is resazurin, a non-toxic and cell-permeable dye. Resazurin (blue and non-fluorescent) is reduced to resorufin (pink and fluorescent) in metabolically active cells. This colorimetric change allows indirect measurement of cell viability[26,27]. The more active the cells are, the greater the reduction of resazurin, resulting in a more intense colour change and increased absorbance at 570nm.

The alamarBlue reagent (DAL1100, Invitrogen) was diluted 1:10 in F-12 cell culture media and 100 µL were pipetted into the wells. Plates were then analysed using a plate reader (Agilent BioTek Synergy HTX Multi-Mode Microplate Reader). The absorbance of alamarBlue was monitored at 570nm, using 600 nm as a reference wavelength. This measurement at two wavelengths enables background correction, improving the reliability of the metabolic activity quantification.

Absorbance was measured at two time points (0h and 2h) to monitor the progression of the metabolic reduction of the reagent. Between measurements, plates were incubated at 37°C to maintain optimal conditions for cell metabolism.

ELISA for IL-6 and MMP1 quantification

In this study, ELISA analysis was used to quantify two key SASP components in the supernatant of treated cells: Interleukin-6 and Matrix Metalloproteinase-1.

A senomorphic compound is expected to reduce the levels of these secreted factors without inducing cell death, thus modulating the inflammatory environment associated with senescent cells.

To perform the ELISA, protocols from the Human IL-6 ELISA Kit (EH2IL6, Thermo Fisher Scientific) and Human MMP1 Elisa Kit (EHMMP1X5, Thermo Fisher Scientific) were followed. 15 µL of each sample supernatant were used for this analysis and diluted accordingly with F-12 medium or assay diluent.

For the IL-6 ELISA, 50 µL of biotinylated antibody reagent and 50 µL of diluted sample or standards were pipetted into each well. The plate was covered and left at room temperature for two hours. After incubation, the plate was washed three times and 100 µL of Streptavidin-HRP solution were added. The plate was covered again and, after 30 minutes of incubation, it was washed three times. Afterwards, 100 µL of TMB substrate were added to each well and incubated in the dark for 30 minutes. Finally, the reaction was stopped by adding 100 µL of Stop Solution, and absorbance was measured at 450 and 550 nm.

For the MMP1 ELISA, 100 µL of the diluted sample or standard curve were added to the wells, followed by 2.5 hours of incubation. The plate was then washed four times and 100 µL of biotin conjugate were added. After 1 hour incubation at room temperature, 100 µL of streptavidin-HRP solution were added, and the plate was covered and incubated in the dark for 30 minutes. Finally, stop solution was added and absorbance was read at 450nm.

Worm Screening

Preparation of S-Buffer

S-buffer was essential for the washing, handling, and synchronization of *C. elegans* populations throughout the experiments. It provided an isotonic environment that maintained worm viability during procedures such as bleaching and transfer.

To prepare 1 L of S-buffer, 129 mL of 0.05 M K_2HPO_4, 871 mL of 0.05 M KH_2PO_4, and 5.85 g of Sodium Chloride (NaCl) were mixed in a sterile Schott glass bottle. The solution was then filled up to 1000 mL with distilled water (dH_2O), autoclaved to ensure sterility, and stored at room temperature until use.

Preparation of Nematode Growth Medium (NGM) Plates

An adequate growth environment for *C. elegans* was essential for the correct screening of the compounds.

To prepare a bottle of 500 mL of NGM, 1.25g Tryptone/Peptone from Casein, 1.5g of Sodium Chloride ≥99.0% and 500 mL RO-H2 were mixed using a magnetic stirrer. Then, 8.5g of Bacteriological-grade Agar was added. Finally, the mixture was autoclaved to ensure sterility and stored at room temperature.

Prior to its use, the NGM-Agar bottle was melted in the microwave and equilibrated to ~50°C in the water bath. Next, the following reagents were added to the bottle: 500 µL Cholesterol/Ethanol (5 mg/mL in 95% EtOH), 500 µL 1 M MgSO4, 500 µL 1 M CaCl2 and 12.5 mL 1 M filtered KPO4. Lastly, 150µL of this mixture was pipetted into each well in a 96 well plate. Plates were stored at 4ºC.

Preparation of LB Medium, Bacterial Culture and NGM Plate Seeding

In this study, *Escherichia coli* (*E. coli*) OP50 was used for *C. elegans* feeding. To ensure a proper bacterial lawn, *E. coli* OP50 was grown and concentrated before seeding onto NGM plates.

The first step was the bacterial cultivation in LB Medium. To prepare 500mL of LB medium, 5g of Tryptone/Peptone from Casein, 2.5g of Yeast Extract and 5g Sodium Chloride (NaCl) were mixed. The pH was adjusted to 7.0 using 1 M Sodium Hydroxide (NaOH). Then, the solution was autoclaved to ensure sterility.

Afterwards, 100 mL of LB medium was inoculated with *E. coli* OP50. The culture was incubated overnight at 37ºC with shaking at 150 rpm.

Bacteria was then combined and concentrated 20X to ensure the dense bacterial lawn for the proper feeding of *C. elegans*.

15 µL of 20X *E. coli* OP50 was pipetted into each well in a 96-well NGM plate. Plates were then centrifuged at 1000 rpm for 1 minute. The centrifugation restricts the bacterial lawn to the centre in order to minimize worm escape. Plates were left at room temperature inside the hood to dry.

Finally, bacteria were inactivated using UV light in a cross-linker for approximately 15 minutes. Plates were stored at 4ºC.

Bleaching Procedure and *C. elegans* Seeding

C. elegans strain TJ1060 was used in this study. This strain carries two temperature-sensitive mutations: spe-9(hc88) I and rrf-3(b26) II[28]. These mutations abolish sperm production, making the worms completely sterile at 25ºC, while still allowing progeny production when cultured at lower temperatures (15-20ºC)[29]. This feature was particularly useful for this study, as it prevented progeny contamination on the plates without the need of chemical sterilization methods such as FUDR, which can potentially alter lifespan[30].

In order for compounds to be tested, it was necessary to ensure all worms were synchronized in the L1 larval stage. To achieve this synchronization, a bleaching procedure was used. Worms were harvested by washing stock plates containing gravid hermaphrodites with 8mL of S-buffer, and collecting the liquid in a falcon tube. Then, 1 ml of 6.25M NaOH and 1mL of bleaching solution (5-7% solution of sodium hypochlorite - NaClO) were added. The falcon tube was vortexed briefly every two minutes for a total of ten minutes. Maximum time did not exceed 10 minutes to avoid reducing the egg viability.

The tube was next centrifuged at 1000rpm for one minute to precipitate the released eggs. Most of the supernatant was removed, and the pellet was resuspended in 9ml of fresh S-buffer. These two steps were repeated seven times in order to dilute and eliminate residual NaOH and bleach. The falcon tube was then left overnight at 20ºC to allow the eggs to hatch and obtain synchronized L1 larvae.

The following day, the suspension was centrifuged and the volume was reduced to achieve a concentration of approximately 10 L1 larvae per 10µL. The synchronized larvae were then ready to be seeded into NGM plates.

To seed the *C. elegans* into 96-well plates, 10µL of L1 larvae suspension were pipetted into each well, containing solid NGM media and bacteria. Only the central wells of the plate were used, leaving the wells around the edges empty to avoid drying effects. The liquid was allowed to evaporate in the hood and plates when then incubated at 25ºC to prevent egg-laying.

Compound Testing

After 2.5 days of incubation, worms reached adulthood and compounds could be added. Each compound was diluted in sterile S-buffer at the desired concentrations. A maximum of 15 µL of the compound solution was incorporated to each well, ensuring the added liquid did not exceed 10% of the media volume. The liquid was allowed to dry for 3-4 hours. Then, plates were incubated at 25ºC.

Every 2-3 days, worm viability was assessed by gently taping the plate on a flat surface and observing under a microscope. Only moving worms were considered alive.

ACKNOWLEDGMENTS

I would like to express my gratitude to Dr. Markus Schosserer for giving me the opportunity to carry out my internship in his laboratory at the Institute for Medical Genetics. His guidance and expertise made the experience especially enriching. I am also thankful to all the members of the Schosserer Lab for their support, kindness, and motivation during my time there. I am especially grateful to Raúl López Galisteo for his dedication as my supervisor throughout this project. His advice, patience and encouragement made a significant impact on both my work and learning experience. I would also like to thank Dr. Ana Palanca Cuñado for her help as my thesis supervisor. Finally, I want to thank my family and friends for their constant support throughout my studies.

BIBLIOGRAPHY

1. Zhang, L., Pitcher, L.E., Prahalad, V., Niedernhofer, L.J., and Robbins, P.D. (2023). Targeting cellular senescence with senotherapeutics: senolytics and senomorphics. FEBS J 290, 1362–1383. https://doi.org/10.1111/FEBS.163.

2. López-Otín, C., Blasco, M.A., Partridge, L., Serrano, M., and Kroemer, G. (2013). The hallmarks of aging. Cell 153, 1194-1217. https://doi.org/10.1016/j.cell.2013.05.039.

3. Guo, J., Huang, X., Dou, L., Yan, M., Shen, T., Tang, W., and Li, J. (2022). Aging and aging-related diseases: from molecular mechanisms to interventions and treatments. Signal Transduction and Targeted Therapy 7:1 7, 1-40. https://doi.org/10.1038/s41392-022-01251-0.

4. Baechle, J.J., Chen, N., Makhijani, P., Winer, S., Furman, D., and Winer, D.A. (2023). Chronic inflammation and the hallmarks of aging. Mol Metab 74, 101755 https://doi.org/10.1016/J.MOLMET.2023.101755.

5. López-Otín, C., Blasco, M.A., Partridge, L., Serrano, M., and Kroemer, G. (2023). Hallmarks of aging: An expanding universe. Cell 186, 243–278. https://doi.org/10.1016/J.CELL.2022.11.001.

6. Ovadya, Y., and Krizhanovsky, V. (2014). Senescent cells: SASPected drivers of age-related pathologies. In Biogerontology (Kluwer Academic Publishers), pp. 627–642. https://doi.org/10.1007/S10522-014-9529-9/METRICS.

7. Zhang, L., Pitcher, L.E., Yousefzadeh, M.J., Niedernhofer, L.J., Robbins, P.D., and Zhu, Y. (2022). Cellular senescence: a key therapeutic target in aging and diseases. J Clin Invest 132. https://doi.org/10.1172/JCI158450.

8. Kumari, R., and Jat, P. (2021). Mechanisms of Cellular Senescence: Cell Cycle Arrest and Senescence Associated Secretory Phenotype. Front Cell Dev Biol 9, 645593. https://doi.org/10.3389/FCELL.2021.645593/XML/NLM.

9. Institute for Health Metrics and Evaluation (2024). Global life expectancy to increase by nearly 5 years by 2050 despite geopolitical, metabolic, and environmental threats, reports new global study. Institute for Health Metrics and Evaluation. https://www.healthdata.org/news-events/newsroom/news-releases/global-life-expectancy-increase-nearly-5-years-2050-despite.

10. Gerasymchuk, M., Robinson, G.I., Kovalchuk, O., and Kovalchuk, I. (2022). Modeling of the Senescence-Associated Phenotype in Human Skin Fibroblasts. Int J Mol Sci 23, 7124. https://doi.org/10.3390/IJMS23137124/S1.

11. Zhang, S., Li, F., Zhou, T., Wang, G., and Li, Z. (2020). Caenorhabditis elegans as a Useful Model for Studying Aging Mutations. Front Endocrinol (Lausanne) 11. https://doi.org/10.3389/FENDO.2020.554994.

12. Bulterijs, S., and Braeckman, B.P. (2020). Phenotypic Screening in C. elegans as a Tool for the Discovery of New Geroprotective Drugs. Pharmaceuticals 2020, Vol. 13, Page 164 13, 164. https://doi.org/10.3390/PH13080164.

13. Novais, E.J., Tran, V.A., Johnston, S.N., Darris, K.R., Roupas, A.J., Sessions, G.A., Shapiro, I.M., Diekman, B.O., and Risbud, M. V. (2021). Long-term treatment with senolytic drugs Dasatinib and Quercetin ameliorates age-dependent intervertebral disc degeneration in mice. Nat Commun 12. https://doi.org/10.1038/s41467-021-25453-2.

14. Yousefzadeh, M.J., Zhu, Y., McGowan, S.J., Angelini, L., Fuhrmann-Stroissnigg, H., Xu, M., Ling, Y.Y., Melos, K.I., Pirtskhalava, T., Inman, C.L., et al. (2018). Fisetin is a senotherapeutic that extends health and lifespan. EBioMedicine 36, 18–28. https://doi.org/10.1016/j.ebiom.2018.09.015.

15. Baker, D.J., Childs, B.G., Durik, M., Wijers, M.E., Sieben, C.J., Zhong, J., A. Saltness, R., Jeganathan, K.B., Verzosa, G.C., Pezeshki, A., et al. (2016). Naturally occurring p16 Ink4a-positive cells shorten healthy lifespan. Nature 530, 184–189. https://doi.org/10.1038/nature16932.

16. Raffaele, M., and Vinciguerra, M. (2022). The costs and benefits of senotherapeutics for human health. Lancet Healthy Longev 3, e67–e77.

17. Morsli, S., and Bellantuono, I. (2021). The use of geroprotectors to prevent multimorbidity: Opportunities and challenges. Mech Ageing Dev 193, 111391. https://doi.org/10.1016/J.MAD.2020.111391.

18. Hajighasemi, F., and Tajik, S. (2017). Hajighasemi F et al. Assessment of Cytotoxicity of Dimethyl Sulfoxide in Human Hematopoietic Tumor Cell Lines.

19. Najari Beidokhti, M., Villalba, N., Ma, Y., Reynolds, A., Villamil, J.H., and Yuan, S.Y. (2025). Lung endothelial cell senescence impairs barrier function and promotes neutrophil adhesion and migration. Geroscience. https://doi.org/10.1007/s11357-025-01517-9.

20. Bitencourt, T.C., Vargas, J.E., Silva, A.O., Fraga, L.R., and Filippi-Chiela, E. (2024). Subcellular structure, heterogeneity, and plasticity of senescent cells. Aging Cell 23, e14154. https://doi.org/10.1111/acel.14154.

21. Henderson, B., Kaiser, F., and Kaiser, F. (2013). Do reciprocal interactions between cell stress proteins and cytokines create a new intra-/extra-cellular signalling nexus? Cell Stress Chaperones 18, 685–701. https://doi.org/10.1007/s12192-013-0444-9.

22. Payea, M.J., Dar, S.A., Anerillas, C., Martindale, J.L., Belair, C., Munk, R., Malla, S., Fan, J., Piao, Y., Yang, X., et al. (2024). Senescence suppresses the integrated stress response and activates a stress-remodeled secretory phenotype. Mol Cell 84, 4454-4469.e7. https://doi.org/10.1016/j.molcel.2024.10.003.

23. Lee, S.J., and Kenyon, C. (2009). Regulation of the Longevity Response to Temperature by Thermosensory Neurons in Caenorhabditis elegans. Curr Biol 19, 715. https://doi.org/10.1016/J.CUB.2009.03.041.

24. Beck, J., Horikawa, I., and Harris, C. (2020). Cellular Senescence: Mechanisms, Morphology, and Mouse Models. Vet Pathol 57, 747–757.

25. BioLegend (n.d.). Live/Dead Cell Discrimination. BioLegend Technical Resource. https://www.biolegend.com/live_dead.

26. Rampersad, S.N. (2012). Multiple applications of Alamar Blue as an indicator of metabolic function and cellular health in cell viability bioassays. Sensors (Basel) 12, 12347–12360. https://doi.org/10.3390/S120912347.

27. Alamar Biosciences (n.d.). alamarBlue® Assay: Indications for Use and Technical Information. Alamar Biosciences.

28. Wormbase (n.d). TJ1060 (strain) - WormBase : Nematode Information Resource https://wormbase.org/species/c_elegans/strain/WBStrain00034903#03--10.

29. Lucanic, M., Garrett, T., Gill, M.S., and Lithgow, G.J. (2018). A simple method for high throughput chemical screening in caenorhabditis elegans. Journal of Visualized Experiments 2018. https://doi.org/10.3791/56892.

30. Angeli, S., Klang, I., Sivapatham, R., Mark, K., Zucker, D., Bhaumik, D., Lithgow, G.J., and Andersen, J.K. (2013). A DNA synthesis inhibitor is protective against proteotoxic stressors via modulation of fertility pathways in Caenorhabditis elegans. Aging (Albany NY) 5, 759. https://doi.org/10.18632/AGING.100605.

Trabajo de Fin de Grado
Grado en Ciencias Biomédicas · Facultad de Medicina
2024 – 2025

Supplementary Information

Screening for senolytic and senomorphic compounds in HDF76 and their effects as geroprotectors in C. elegans

Sybila Sanguinet Rumayor[1,2], Ana Palanca Cuñado[2,3], Markus Schosserer[1*]

UC | Universidad de Cantabria

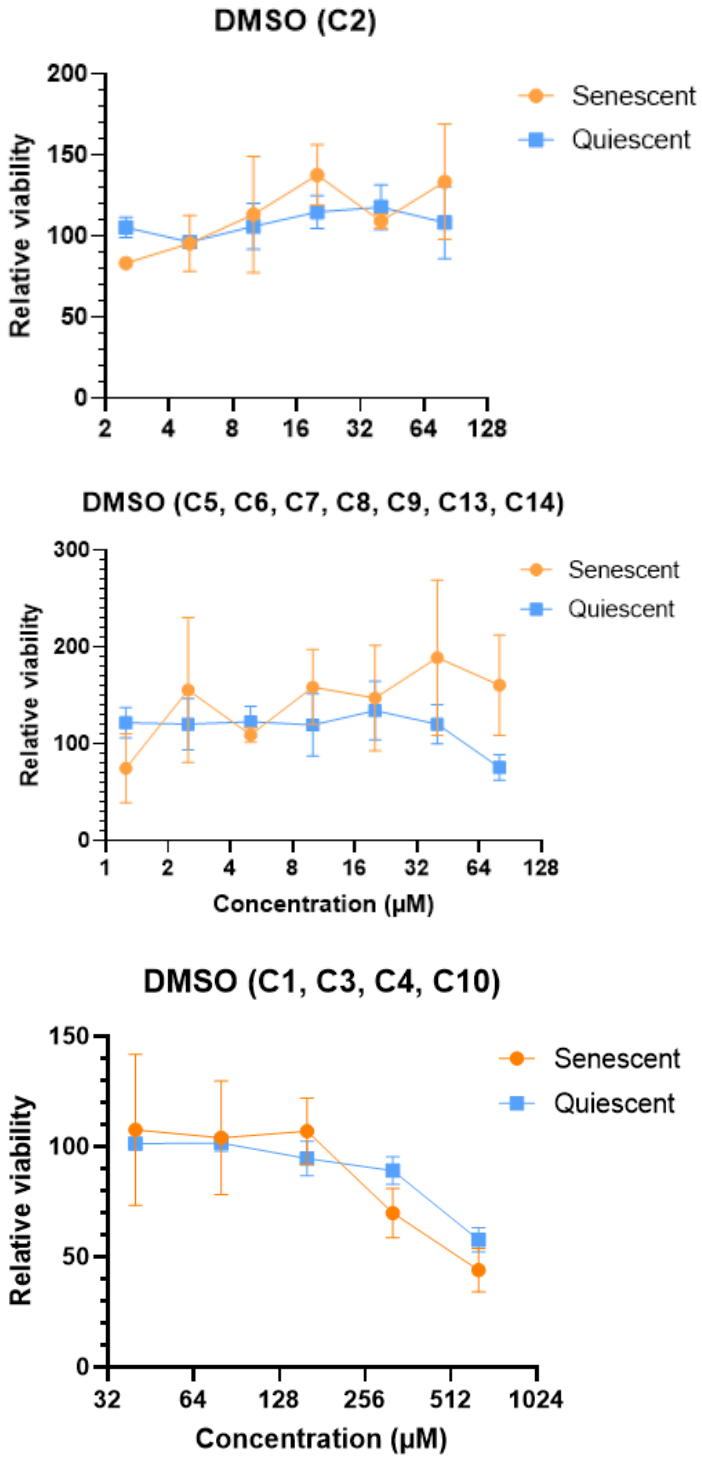

Figure S1. DMSO controls of the Alamar Blue Assays

Line graphs showing relative viability of senescent and quiescent HDF76 treated with DMSO as a control. **(A)** DMSO control for compound 2 **(B)** DMSO control for compounds 5, 6, 7, 8, 9, 12 and 13 **(C)** DMSO controls for compounds 1, 3, 4 and 10.

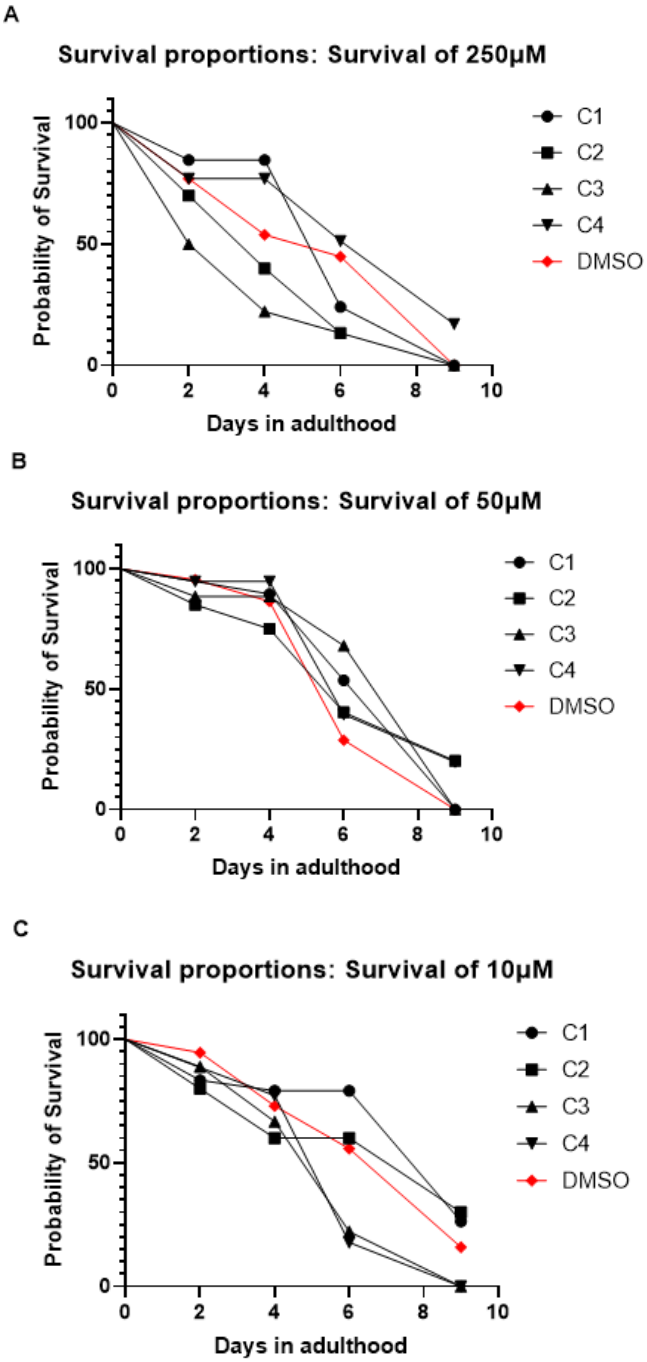

Figure S2. Survival analysis in *C. elegans*.

Line graphs showing the survival of C. elegans in the first experiment, where worms were kept in an incubator at 27ºC. All worms died prematurely by day 9, regardless of treatment, indicating that excessive temperature led to accelerated mortality. *C. elegans* were treated with compounds 1, 2, 3 and 4 at concentrations **(A)** 250µM **(B)** 50µM and **(C)** 10µM. No significant differences were observed between the compound-treated groups and the DMSO controls at any concentration ($p > 0.05$, Log-rank (Mantel-Cox) test).